*Revista Mexicana de Astronomía y Astrofísica*, **60**, 165–175 (2024)

https://doi.org/10.22201/ia.01851101p.2024.60.01.12

# ASTRONOMICAL SIGNALS IN THE BRIGHTEST FIREBALLS THAT FALL ON EARTH

D. Maravilla[1], M. Pazos[2], and G. Cordero[1]

*Received January 25 2023; accepted February 2 2024*

ABSTRACT

In this work a wavelet spectral study of a time series of brightest fireballs is presented. The wavelet analysis shows that are two solar periodicities around 27 and 13.5 days. These periodicities have been associated to Carrington rotation and lunar motions and indicate that both Solar and Lunar rotations could have an influence on the brightest fireballs that fall on Earth. A third periodicity around 2.5 days was also identified in almost all spectra but it could be a harmonic of those periods.

RESUMEN

En este trabajo se presenta un estudio espectral de series de tiempo de la entrada de meteoroides pequeños a la atmósfera terrestre usando la técnica wavelet. El análisis muestra que hay dos señales alrededor de 27 y 13.5 días. Estas periodicidades han sido asociadas a la rotación Carrington y a los periodos lunares que podrían estar influenciando la caída de este tipo de objetos sobre la Tierra. Una tercera periodicidad alrededor de 2.5 días fue identificada en casi todos los espectros obtenidos y podría ser una señal armónica de las periodicidades lunar y solar.

*Key Words:* meteorites, meteors, meteoroids — Moon — Sun: rotation



## 1. INTRODUCTION

There are many phenomena that can be observed in the atmosphere of our planet, from the formation of clouds to the arrival of bodies that come from space and cross the different layers of the atmosphere, producing luminous phenomena such as meteors and meteor showers. An average of 100,000 metric tons of material from space arrives on Earth yearly (Brownlee 2001; Trigo-Rodríguez 2019). Part of this material ablates in the atmosphere while the rest can survive and be deposited as meteorites on the Earth's surface, at the bottom of the oceans or on the ice of Antarctica, where it can be collected. A particular case of extraterrestrial material that reaches Earth are dust particles (IDPs), also called Brownlee particles, which can remain suspended in the stratosphere and be collected by planes to be analyzed in laboratories (Duprat et al. 2007) or become embedded in spacecrafts where they impact (Moorhead et al. 2020). The IDPs contain information on the compounds that come from the cloud of gas and dust that gave rise to our Solar System, as well as information from the pre-solar period. These bodies come mainly from comets and probably from asteroids (Bradley et al. 1996; Vernazza et al. 2015).

From recent studies carried out on meteorites it is known that much of the extraterrestrial material comes mainly from undifferentiated bodies, small asteroids and comets (Trigo-Rodríguez 2019). In particular, it has been observed that the extraterrestrial material that reaches the surface of our planet is mainly of a chondritic nature. On the other hand, material that has an origin in differentiated bodies can also reach Earth, as is the case of achondritic meteorites whose origin may be Mars, as the ALH84001 meteorite (McKay et al. 1996; McSween & Harry 1996), the asteroid Vesta from which the Tatahouine meteorite comes from (Maravilla et al. 2013) or the Moon, as the lunar meteorites found and collected in Northern Africa (Korotev & Irving 2021; Heiken et al. 1991).

A particularity of asteroids and comets is that they are constantly subjected to erosion processes, which makes them one of the main sources of meteoroids that form the zodiacal cloud. While aster-

[1]Instituto de Geofísica, UNAM, México.
[2]Instituto de Cambio Climático, y Ciencias de la Atmósfera, UNAM, México.

oidal meteoroids are produced by impacts, cometary meteoroids come from the degassing of their parent bodies (Jenniskens 1998; Trigo-Rodríguez 2019) considering that comets were formed in distant regions of the protoplanetary disk from the accretion of primordial materials made up of ice, organic material and dust grains (Trigo-Rodríguez & Blum 2022), and asteroids were formed in the inner solar system and are made up fundamentally of minerals (JPL NASA CNEOS: NEO Basics, https://cneos.jpl.nasa.gov/fireballs/). When comets approach the Sun, they sublimate, generating jets that emit large quantities of meteoroids into space. These meteoroids form beams of dust that can remain in stable orbits around the Sun for thousands of years (Williams 2002) and can be intercepted by planets such as the Earth. To exemplify this fact, the Earth receives tens of kilograms of material that comes from meteor showers such as the Leonids or the Perseids (Trigo-Rodríguez & Blum 2009) that have their origin in the comets 55P/Tempel- Tuttle and 109P/Swift-Tuttle respectively.

In recent years, it was discovered by the JUNO space mission that Mars is the main source of dust in the zodiacal cloud between 1 and 2.8 AU (Jorgensen et al. 2020), becoming the third source of material that feeds the zodiacal cloud. When cometary or asteroidal meteoroids impact a planetary atmosphere, they will be decelerated, fragmented, evaporated and/or pulverized. The speed of a meteoroid that impacts the atmosphere is in the range of 11 to 72 km/s. As cometary meteoroids are made up of organic matter, micrometric dust and volatiles, they cannot survive their passage through the atmosphere (Trigo-Rodríguez & Blum 2009). As a result of the collision of a meteoroid with the atmosphere, ionization, ablation, fragmentation and light generation can occur (fireballs) (Trigo-Rodríguez 2019; Mas Sanz et al. 2020).

Trigo-Rodríguez & Blum (2022) presented the results of an investigation based on the study of meteoroid stream flux and mass distribution of cometary material that arrives on Earth. The fundamental results of this work show that there is a gap between the mass distribution of cometary dust and the largest IDPs collected in the atmosphere, and show that the typical sizes of cometary meteoroids (3 cm) cannot survive their passage through the atmosphere; but if fragmentation occurs in the upper atmosphere, then the meteoroids may not undergo ablation and therefore some of the IDPs could be fragments of low-velocity meteoroids. The results also indicate that the direct flow coming from the meteoroid streams has a minor contribution from cometary meteoroids accreting on the Earth (of the order of 500 tons/y). The same work also mentions that comets could have participated in the massive delivery of sodium and organic compounds to the early Earth.

The study from a scientific point of view of the extraterrestrial material that reaches our planet has been carried out since the last century through the construction of observation networks, detection instruments and monitoring networks; highlights are the US Government sensors (USG) that have documented the entry of fireballs around the world since 1988 (Tagliaferri et al. 1994) and the worldwide FRIPON network, which has monitored the entry of 4000 meteoroids since 2016 (Colas et al. 2020) above part of western Europe and characterized its physical and dynamic properties. With this network, the flux of meteorites larger than 100g has been estimated, being of the order of $14/\mathrm{yr}/10^6$ km$^2$. According to Ceplecha et al. (1998) and Rubin & Grossman (2010), once a body coming from the interplanetary medium travels across the terrestrial atmosphere, it can produce a luminous phenomenon called meteor if its size is larger or equal than 100 microns. Fireballs are meteors whose magnitude is $-4$ or brighter (Blanch et al. 2017). This phenomenon can be registered by different instrument such as optical telescopes, radar, lidar, and infrasound sensors (Edwards et al. 2005; Brown et al. 2008; Trigo-Rodríguez et al. 2008).

Peña-Asensio et al. (2022) reported the orbits of the meter-sized hazardous projectiles that impacted the Earth's atmosphere and investigated the possible connection that the projectiles could have with cometary and asteroidal meteoroid streams and NEO's ( Near Earth Objects). The authors used the series of superbolide events from the CNEOS database recorded by the United States Government sensors. Of the 887 events in the database, only 255 were analyzed because they had enough information to calculate their heliocentric orbit. The results of this research indicate that only 58 of the events probably have a cometary or asteroidal origin. These 58 events represent 23 % of the total number of meter-sized projectiles that produce large bolides, which implies that one in four superbolides is originated by near-Earth objects (NEO's). The authors, based on the height and speed of each event in the database (CNEOS), found that 61.9 % of the projectiles are rocky or rocky-iron, 35.7 % are carbonaceous and 2.4 % are cometary. In relation to their heliocentric orbit, 85.5 % have orbital elements similar to

those of asteroids and 9.8 % correspond to comets of the Jupiter family. Of the events analyzed, the researchers identified 5 events with hyperbolic orbits and identified the orbital elements of the first interstellar superbolide detected on January 8, 2014, concluding that at least 1 % of the large meteoroids that impact the Earth's atmosphere could be of interstellar origin.

The Earth and the Moon are under the gravitational and electromagnetic influence of the Sun. The effects on the Earth have been identified through spectral analysis of time series of solar phenomena or events such as sunspots, the magnetic solar cycle or solar cosmic rays. Through spectral analysis using different techniques, several short, medium and long-term periodicities have been identified, ranging from days to years. Some of these periodicities have been identified in terrestrial phenomena from geomagnetic, atmospheric and oceanographic points of view, showing that there is a relationship between the Sun and the Earth. But just as this relationship exists, the Sun has also influence on other bodies of the Solar System, such as meteoroids, comets and asteroids; there is also a strong gravitational influence of the Earth and the Moon on the bodies living in the terrestrial vicinity.

## 2. THE BRIGHTEST FIREBALLS DATA

In this research a time series related to registered fireballs corresponding to the last 33 years is spectrally studied taking into account 852 events with energies greater than 0.073 Kt from 15 April 1988 to 29 December 2020. The data were provided by the United States Government sensors homepage and released to the Near Earth Object Program (https://cneos.jpl.nasa.gov/fireballs/); they contain the following information: peak brightness data/time, geographical location, altitude and speed when the object reaches its maximum brightness, approximate total optical energy and calculated total impact energy.

### 2.1. *The Spectral Method*

When astronomical and astrophysical data are analyzed we can expect gaps or errors due to different record techniques and times (Jopek & Kaňuchová 2017; Soon et al. 2019). Spectral analysis has been used to study time series with missing astronomical and astrophysical data (Feigelson 1997; Scargle 1997; Ding et al. 1998). The Fourier transform (FT) can be applied to analyze the time series. However, this method might not be suitable for non-stationary and irregularly spaced time series; therefore, another method is required to study a time series with gaps such as the brightest fireball events. The classical wavelet technique (Torrence & Compo 1998; Velasco et al. 2017) is used for non-stationary time series. The wavelet method is useful for analyzing local variations of power within a single non-stationary time series at multiple periodicities. We applied this method using the Morlet function specially developed for geophysical phenomena, which provides a good time resolution (Torrence & Compo 1998). We also applied the Morlet mother function to analyze the power spectral density (PSD) of the brightest fireballs, since this mother function does not only provide a higher periodicity resolution but is also a complex function that allows to calculate the inverse wavelet transform (Torrence & Compo 1998; Soon et al. 2011; Velasco et al. 2017; Soon et al. 2019). The meaningful wavelet periodicities with a confidence level greater than 85% must be inside the cone of influence (COI), and the interval of 85% confidence (Torrence & Compo 1998) is marked by thin black contours in the spectra. The global spectra have been included in all wavelet plots to show the power contribution of each periodicity inside the COI (See Figure 1, for example). Also, we established the significance levels in the global wavelet spectra with a simple red noise model where the power increases at lower frequencies (Gilman et al. 1963). The uncertainties are obtained by dividing the maximum peak width and measuring both halves at the base, related to the period scale (Mendoza et al. 2006). By applying this method to the whole time series of the brightest fireballs and using the toolbox developed by Grinstead et al. (2014) we obtained periodicities of different time scales, ranging from days to years. We aimed to focus on periodicities of higher frequency (scale of days), and then we filtered the data with a high pass band filter. The periodicities found with the wavelet method were validated using Redfit-X (Björg Ólafsdóttir, et al. 2016).

## 3. RESULTS AND DISCUSSION

The first wavelet PSD was obtained with the complete time series. Later, this time series was filtered and spectrally analyzed by short intervals consisting of the brightest fireball series related to the ascending and descending phases of the solar cycle. Based on the span of the brightest fireball time series used, we found three short intervals associated with the descending solar phases and corresponding to solar cycles 22, 23 and 24, and two related to the ascending solar phase of solar cycles 23 and 24, respectively. The short time series associated with

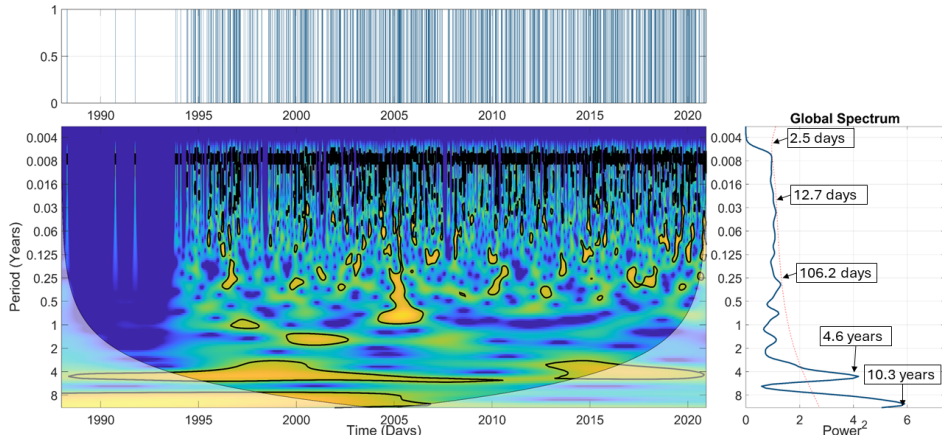


Fig. 1. Wavelet spectrum of the brightest fireball meteor data provided by United States Government sensors from 1988 to 2020. On the right side the global spectrum shows significant periodicities at 2.5, 12.7 and 106.2 days, and 4.6 and 10.3 years. The red dotted line represents the 85 % confidence level. The PSD spectrum is shown in the middle of the figure. The time series of the brightest fireballs is presented above the PSD. The color figure can be viewed online.

the descending solar phases correspond to the following intervals: 1991 to 1996 for solar cycle 22; 2000 to 2008 for solar cycle 23 and 2014 to 2020 for solar cycle 24. The short time series related to the ascending solar phases correspond to the following intervals: 1996 to 2000 for solar cycle 23 and 2008 to 2014 for solar cycle 24.

### 3.1. *Wavelet Analysis*

#### 3.1.1. *The Complete Time Series of the Brightest Fireballs*

The wavelet spectrum of the complete time series of the brightest fireballs shows five significant periodicities (Figure 1) From an inspection of Figure 1, the peak with the hightest power is located at 10.3 years while the next one is at 4.6 years. The other three periodicities are located at 106.2 days, 12.7 days and 2.5 days, respectively (Table 1). All these periodicities are related to an 85% confidence level. Ge (2007), describes accurately that the significance test of the wavelet method developed by Torrence and Compo addresses the issue of how to distinguish statistically significant results from those due to pure randomness when only one sample of the population is studied, as is the case of the time series of fireballs used in this research. The confidence level is also calculated by the program and has been established in the results by the red noise line. The length of the time series and the temporal resolution are related with this level of confidence. The longest and highest resolution of data in a time series increases the confidence level.

TABLE 1

PERIODICITIES OF THE COMPLETE TIME SERIES[a]

| Periodicity | + | - |
|---|---|---|
| 2.5 *d* | 0.9 | 0.25 |
| 12.7 *d* | 5.5 | 3.2 |
| 106.2 *d* | 36.5 | 21.9 |
| 4.6 *y* | 0.9 | 1.15 |
| 10.3 *y* | 1.3 | 4.16 |

[a]The uncertainties are indicated with the signs + and - respectively. Days - d; Years - y.

#### 3.1.2. *Filtered Short Time Series of Brightest Fireballs*

a) Solar descending phases

In order to obtain the PSD spectra, the wavelet technique was used again in all short time series. Figures 2, 3 and 4 show the spectra of the brightest fireball time series associated with the descending phase of solar cycles 22, 23 and 24, respectively. Figure 2 shows the PSD related to solar cycle 22. In this figure two periodicities can be observed around 2.5 and 117 days (Table 2). Only the peak at 117 days is above the 85% confidence level. Figure 3 shows the wavelet PSD spectrum of the brightest fireball meteors linked to the descending solar cycle 23. In this figure it can be seen that there are five periodicities at 3.1, 5.8, 14.7, 22 and 280.1 days (Table 2), all of them under the 85% confidence level. The wavelet PSD spectrum associated with the descending solar phase of solar cycle 24 appears in Figure 4. In this plot, four periodicities appear at 2.5, 7.4, 29.5 and

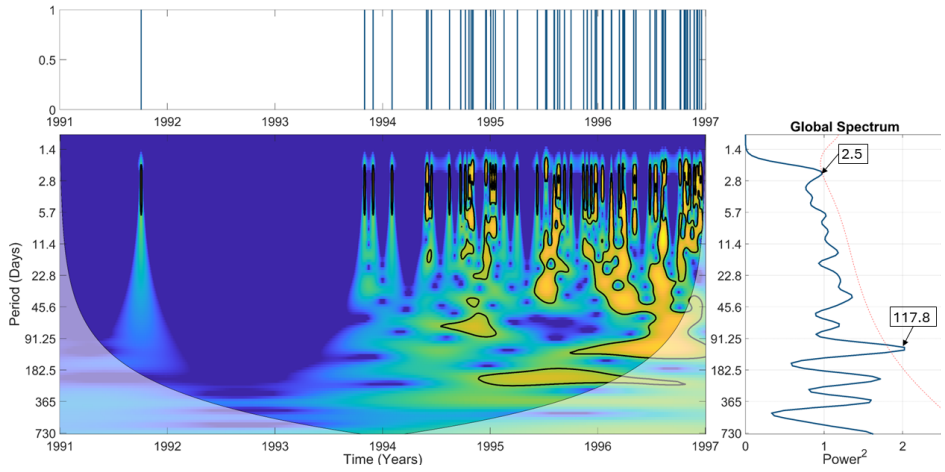


Fig. 2. PSD spectrum of the brightest fireball time series associated to the descending solar phase of solar cycle 22. The red dotted line represents the 85 % confidence level. The color figure can be viewed online.

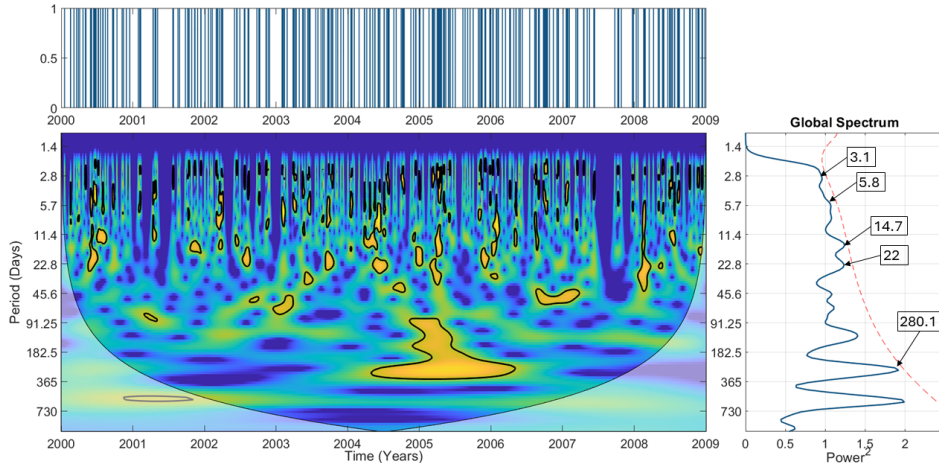


Fig. 3. Wavelet PSD of the brightest fireball time series linked to the solar descending phase of solar cycle 23. All peaks are under the dotted red line that corresponds to the 85 % confidence level. The color figure can be viewed online.

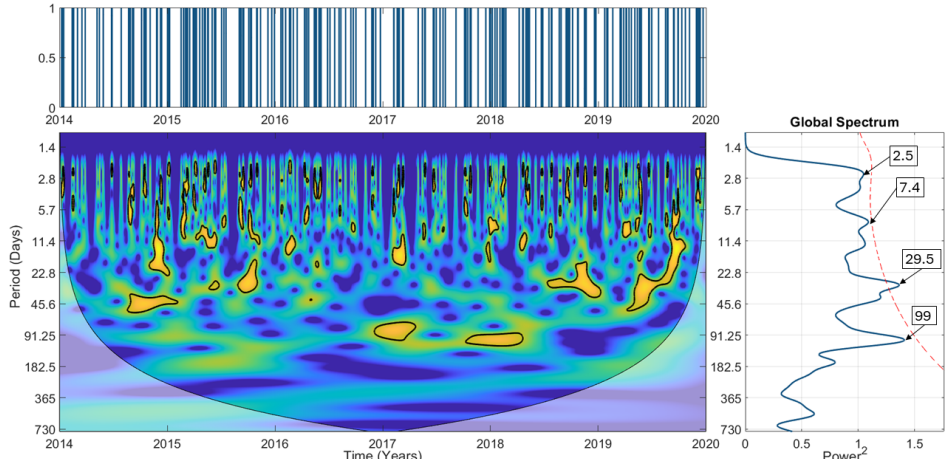


Fig. 4. Wavelet PSD of the brightest fireball time series linked to the descending solar phase of solar cycle 24. All peaks are under the dotted red line that corresponds to the 85 % confidence level. The color figure can be viewed online.

TABLE 2

PERIODICITIES IN SOLAR CYCLES (DESCENDING PHASE[a])

| Solar cycle | Interval (years) | Periodicity (days) | (+) | (-) |
|---|---|---|---|---|
| 22 | 1991 – 1996 | 2.5 | 0.8 | 0.4 |
| ··· | ··· | 117 | 22.3 | 29.5 |
| 23 | 2000 – 2008 | 3.1 | 0.6 | 0.6 |
| ··· | ··· | 5.8 | 0.7 | 0.3 |
| ··· | ··· | 14.7 | 3.9 | 2.3 |
| ··· | ··· | 22.0 | 5.7 | 3.5 |
| ··· | ··· | 280.1 | 93.8 | 82.1 |
| 24 | 2014 – 2020 | 2.5 | 0.8 | 0.2 |
| ··· | ··· | 7.4 | 1.9 | 0.8 |
| ··· | ··· | 29.5 | 7.7 | 3.2 |
| ··· | ··· | 99 | 25.9 | 20.4 |

[a]Uncertainties are indicated with the signs + and - and are stated in days(d).

TABLE 3

PERIODICITIES IN SOLAR CYCLES (ASCENDING PHASE[a])

| Solar cycle | Interval (years) | Periodicity (days) | (+) | (-) |
|---|---|---|---|---|
| 22 | 1988 – 1991 | ··· | ··· | ··· |
| 23 | 1996 – 2000 | 2.6 | 0.3 | 0.3 |
| ··· | ··· | 4.4 | 0.5 | 0.3 |
| ··· | ··· | 12.4 | 2.3 | 2.5 |
| ··· | ··· | 105 | 27.3 | 21.7 |
| 24 | 2008 – 2014 | 2.5 | 0.8 | 0.2 |
| ··· | ··· | 3.7 | 0.6 | 0.6 |
| ··· | ··· | 29.5 | 7.7 | 3.2 |

[a]Uncertainties are indicated with the signs + and - and are stated in days(d).

99 days and only the periodicity around 29.5 days is above the 85% confidence level (Table 2).

b) Solar ascending phases

Figure 5 shows the PSD spectrum of the fireball time series connected with the ascending phase of solar cycle 23. In this plot four periodicities appear at 2.6, 4.4, 12.4 and 105 days (Table 3). The red line represents the 85% confidence level and all peaks are under this line.

The plot associated with the ascending phase of solar cycle 24 is presented in Figure 6 where three periodicities at 2.5, 3.7 and 29.5 days can be seen. Only the last one is above the 85% confidence level. Analyzing the periodicities observed in Figure 1 and considering uncertainties, the peak at 12.7 days could be linked to the Carrington rotation (27.275 days) as well as to the four Moon periods: synodic, sidereal, nodical or draconic, and anomalistic (SSNA). The synodic period has a duration of 29.531 days, the sideral period has a duration of 27.322 days. The nodical or draconic period is of 27.212 days and the anomalistic month has a duration of 27.555 days (Karttunen et al. 2017). The periodicity at 12.7 days in Figure 1 could be a harmonic of all these periodicities (around 13.5 days). Both the Carrington rotation and the 13.5 days period have been observed in many solar-terrestrial parameters such as sunspot number, solar magnetic emergence, solar wind, the Ca-K-line plage index, sudden storm commencements, and others (Mursula & Zieger 1996; Prabhakaran et al. 2001, 2002, 2004; Emery et al. 2011; Singh & Badruddin 2014). It is important to point out here that the 13.5 days periodicity has also been reported in several scientific papers and is related e.g., to solar wind and ionospheric parameters; its dependence on the solar radiation wavelength has been also found by Donnelly & Puga (1990) and it could be also the lunar periods (SSNA) first harmonic. The peak at 10.3 years could be associated to the sunspots cycle while the peak at 4.6 years may be the first harmonic of that spectral signal. From the spectral analysis of the short time series of the brightest fireball data associated with descending phases of the considered solar cycles (22, 23 and 24), the periodicities at 22 days (solar cycle 23, Figure 3) and at 29.5 days (solar cycle 24, Figure 4) are related to the Carrington rotation period (27.275 days) and the latter periodicity could be associated with the lunar periods (SSNA) if uncertainties are taken into account. In Figure 3, the peak at 14.7 days (solar cycle 23) could have a connection with the solar rotation period (27.275 days) and the Moon periods (SSNA), being its first harmonic. Analyzing the results obtained from the wavelet spectral analysis of the short time series of the brightest fireball data linked to the ascending phases of solar cycles 23 and 24, a peak at 29.5 days is observed in Figure 6 (solar cycle 24), possibly connected with the Carrington rotation and the lunar signals (SSNA), whereas a peak at 12.4 days is observed in Figure 5 (solar cycle 23), which could be a harmonic of the 27.175 days solar rotation and lunar periodicities (SSNA).

Summarizing, the Carrington rotation signal (27.275 days) and the lunar periods (SSNA) are manifested in the spectra of the brightest fireball time series related with descending phases of solar cycles 23 and 24 (Figures 3 and 4) and with the ascending

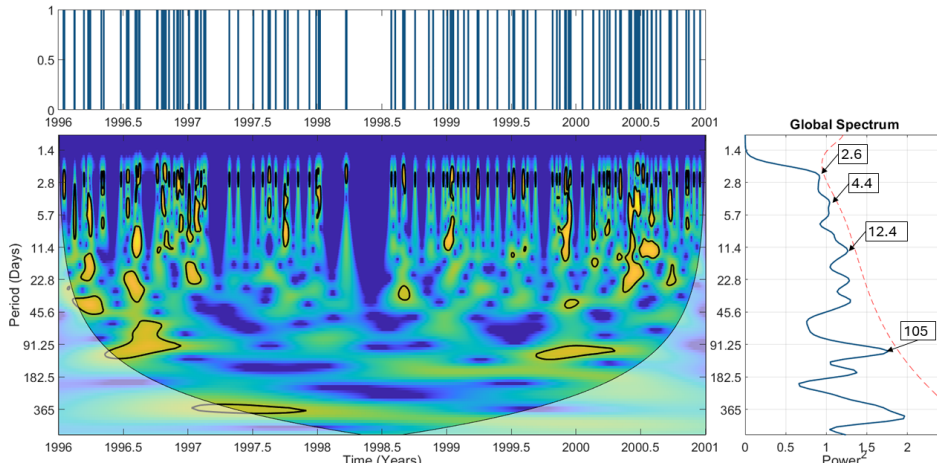


Fig. 5. Wavelet PSD of the brightest fireball time series linked to the solar ascending phase of solar cycle 23. All peaks are under the 85 % confidence level (dotted red line). The color figure can be viewed online.

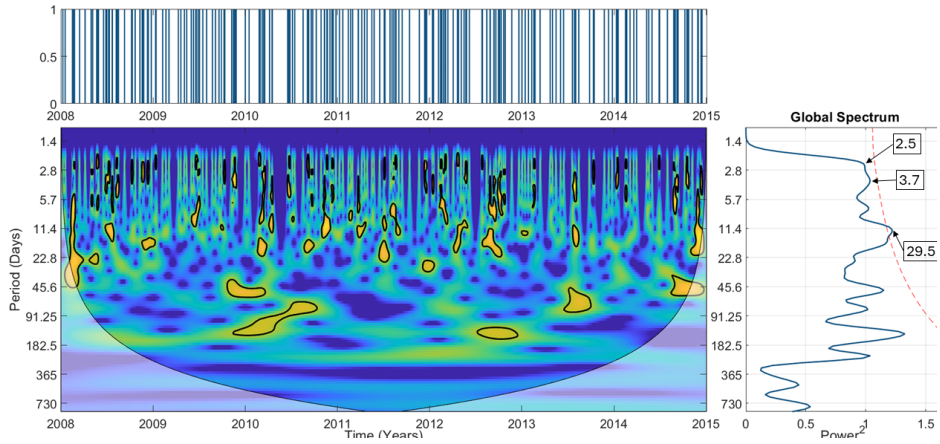


Fig. 6. Wavelet PSD of the brightest fireball time series linked to the solar ascending phase of solar cycle 24. The peak at 29.5 days is above the dotted red line that corresponds to the 85 % confidence level. The color figure can be viewed online.



solar phase of cycle 24 (Figure 6). The first harmonic of the Carrington rotation (13.5 days) could be present in the PSD of the brightest fireball meteor spectra associated with the entire solar cycle 23 (Figures 3 and 5). The presence of a periodicity close to the Carrington rotation period (27.275 days) and the Moon periods (SSNA) in the wavelet spectra of cycles 23 and 24 indicates that the solar rotation and lunar signals have left their mark in the brightest fireballs detected in the terrestrial atmosphere and could be modulating the fall of these extraterrestrial bodies on Earth. Additionally, a periodicity around 2.5 days appears in almost all spectra of the complete and short time series of the brightest fireballs associated with the considered solar cycles (ascending and descending phases), (Tables 2 and 3) although the 3.1 days periodicity in the descending solar phase of solar cycle 23 could be also included here if the uncertainty associated with this peak, is considered. The physical reason for this periodicity is unknown though it could be a minor order harmonic of both the Carrington rotation and the Moon periods.

In order to look for the periodicities we found in the previous analysis (Figures 1-6) and possibly other ones, an additional wavelet analysis was done using the maximum velocity e.g. the entry velocity of meteoroids into the Earth's atmosphere (https://cneos.jpl.nasa.gov/fireballs/). We use the data from 2000 to 2020 because there is no maximum velocity registered before 2000. Separating the max-

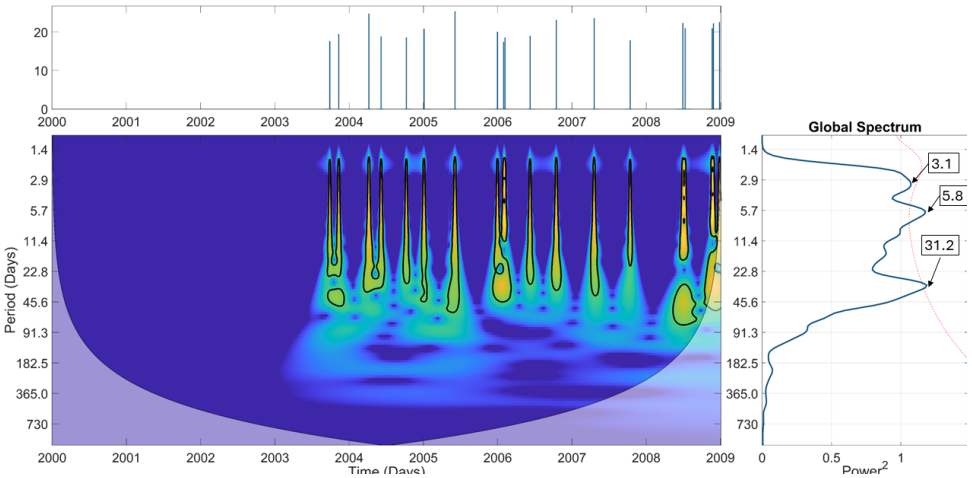


Fig. 7. PSD spectrum of the maximum velocity time series related to solar cycle 23 from 2000 to 2008 years (descending phase). The red dotted line represents the 85 % confidence level. The color figure can be viewed online.

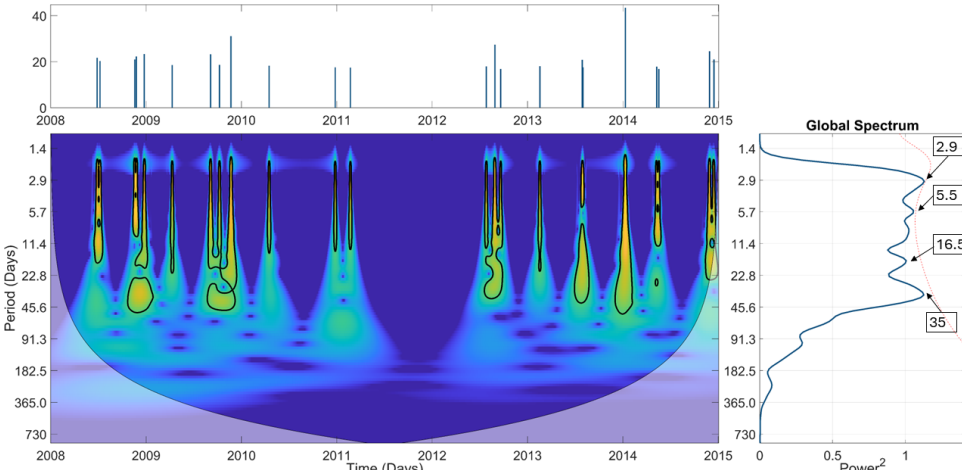


Fig. 8. PSD spectrum of the maximum velocity time series related to solar cycle 24 from 2008 to 2014 years (ascending phase). The red dotted line represents the 85 % confidence level. The color figure can be viewed online.



imum velocity time series based on the solar cycle length, three different intervals were selected corresponding to two descending solar phases from 2000 to 2008 (solar cycle 23) and from 2014 to 2020 (solar cycle 24), (Figures 7 and 9) and one ascending solar phase from 2008 to 2014 (solar cycle 24), (Figure 8), (Table 4).

In the descending period from 2000 to 2008, three periodicities are present at 3.1 days, 5.8 days and 31.2 days, while in the descending period from 2014 to 2020, the periodicities we found are located at 2.8 days, 4.4 days, 6.9 days and 19.7 days. In the ascending phase from 2008 to 2014, five different periodicities were identified, at 2.9 days, 5.5 days, 8.7 days, 16.5 days and 35 days respectively. Taking into account the uncertainties, the lunar periods (SSNA) and the Carrington rotation period (27.275 days) are present in the descending solar phase from 2000 to 2008 and in the interval from 2008 to 2014, corresponding to an ascending solar phase. Analyzing these results from the spectral wavelet analysis we note that regarding the periodicity we observe in solar cycle 23 (Figure 7) at 31.2 days (solar descending phase), the periodicity at 35 days in solar cycle 24 (Figure 8), (solar ascending phase) and the periodicity at 19.7 days in the descending phase of solar cycle 24, all of them could be related to the Moon periods (SSNA) as well, if we consider the uncertainties. The other periodicities (Table 4) could be minor order harmonics of these last periods. If we assume that

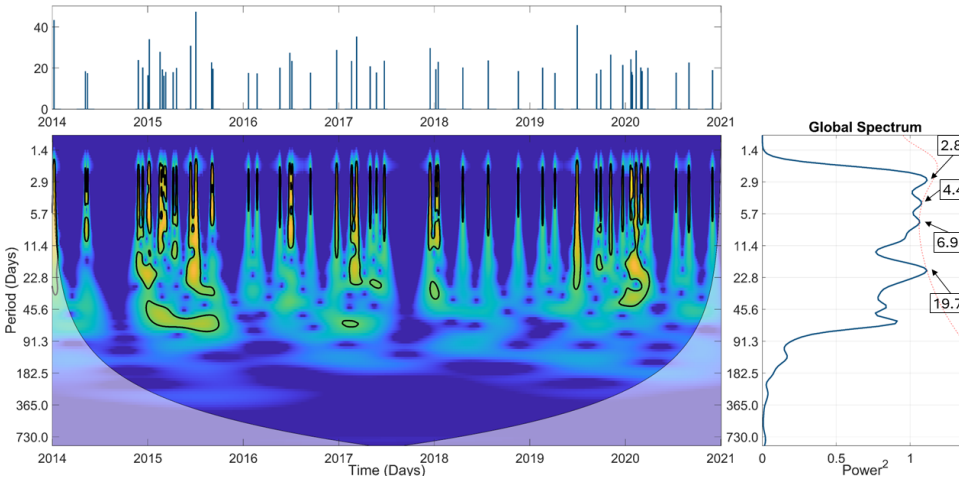


Fig. 9. PSD spectrum of the maximum velocity time series related to solar cycle 24 from 2014 to 2020 years (descending phase). The red dotted line represents the 85 % confidence level. The color figure can be viewed online.

TABLE 4

PERIODICITIES IN THE VELOCITY VECTOR TIME SERIES[a]

| Solar cycle | Interval (years) | Periodicity (days) | (+) | (-) |
|---|---|---|---|---|
| 23 descending phase | 2000 − 2008 | 3.1 | 1.27 | 0.78 |
| ... | ... | 5.8 | 2.96 | 1.42 |
| ... | ... | 31.2 | 12.92 | 6.44 |
| 24 ascending phase | 2008 − 2014 | 2.9 | 1.48 | 0.6 |
| ... | ... | 5.5 | 1.1. | 0.9 |
| ... | ... | 8.7 | 3.7 | 1.3 |
| ... | ... | 16.5 | 5.6 | 2.6 |
| ... | ... | 35 | 9.1 | 11.6 |
| 24 descending phase | 2014 − 2020 | 2.8 | 0.7 | 0.5 |
| ... | ... | 4.4 | 1.1 | 0.7 |
| ... | ... | 6.9 | 1.9 | 1.1 |
| ... | ... | 19.7 | 11.5 | 5.0 |

[a]Uncertainties are indicated with the signs + and − and are stated in days(d).

the fireballs that arrive to our planet could be associated with a potential source of meter-size projectiles as is the case of Near Earth Objects (NEO's), (Peña-Asensio et al. 2022) and since NEO's are closer to the Moon, our satellite has a strong gravitational influence on the NEO's dynamics and the lunar signals are present in the time series analyzed, as shown in the wavelet spectra.

Peña-Asensio et al. (2022) reported that 'certain meteoroid streams' could be another important source of meter-sized hazardous projectiles; then, meteoroid streams could have a significant role as a source of fireballs arriving to Earth as is the case of fragments of comets and asteroids. One example of this are the Taurids (streams and showers) that have been associated not only with NEO's but also with a cometary origin. In this case the comet associated is 2P/Encke (Peña-Asencio et al. 2022).

## 4. CONCLUSIONS

1. A periodicity around 27 days was found in the time series of the brightest fireball meteors, indicating that the Carrington rotation and the Moon (SSNA periods) are modulating the fall of meteors on Earth.

2. The periodicity around 13.5 days is barely present in several wavelet spectra of the short fireballs time series. This periodicity could be a harmonic of the main peak observed around the Carrington rotation and the Moon periods (SSNA), respectively.

3.- The periodicities found around 30 days in the maximum velocity analysis are close to both the Carrington rotation and the lunar periods (SSNA).

4. A peak at 2.5 days was found in almost all spectra (brightest fireball time series) and could be a small harmonic of the Carrington rotation period and lunar signals. On the other hand, this peak is under the 85% confidence level in all spectra of the short time series and is only significant considering the complete time series (Figure 1).

5.- Because most of the fireballs used for the wavelet analysis are less than 10 meters in size, they are not affected by the Yarkovsky effect, but they could be affected by radiation pressure or by the periodical gravity force of the Moon.

## REFERENCES


Björg Ólafsdóttir, K., Schulz, M., & Mudelsee, M. 2016, Comp. & Geosci., 91, 11

Blanch, E., Trigo-Rodríguez, J. M., Madiedo, J. M., et al. 2017, in Assessment and Mitigation of Asteroid Impact Hazards, ed. J. M. Trigo-Rodríguez, M. Gritsevich & H. Palme (Switzerland: Springer), 185

Bradley, J. P., Keller, L. P., Brownlee, D. E., & Thomas, K. L. 1996, M&PS, 31, 394, https://doi.org/10.1111/j.1945-5100.1996.tb02077.x

Brown, P., Weryk, R. J., Wong, D. K., & Jones, J. 2008, in Advances in Meteoroid and Meteor Science, ed J. M. Trigo-Rodríguez, F. J. M. Rietmeijer, J. Llorca, & D. Janches (New York, NY: Springer), 209

Brownlee, D. E. 2001, in Accretion of Extraterrestrial Matter Throughout Earth's History, ed B. Peucker-Ehrenbrink & B. Schmitz (New York, NY: Kluwer Academic/Plenum Publishers)

Ceplecha, Z., Borovička, J., Elford, W. G., et al. 1998, SSRv, 84, 327, https://doi.org/10.1023/A:1005069928850

Colas, F., Zanda, B., Bouley, S., et al. 2020, A&A, 644, 53, https://doi.org/10.1051/0004-6361/202038649

Ding, Y. R., Zhao, H., & Li, Z. Y. 1998, ChA&A, 22, 235, https://doi.org/10.1016/S0275-1062(98)00032-0

Donnelly, R. F. & Puga, L. C. 1990, SoPh, 130, 369, https://doi.org/10.1007/BF00156800

Duprat, J., Engrand, C. Maurette, M. et al. 2007, AdSpR, 39, 605, https://doi.org/10.1016/j.asr.2006.05.029

Edwards, W. N., Brown, P., & Revelle, D. O. 2005, in Modern Meteor Science. An Interdisciplinary View, ed. R. Hawkes, I. Mann, & P. Brown (Dordrecht: Springer)

Emery, B. A., Richardson, I. G., Evans, D. S., Rich, F. J., & Wilson, G. R. 2011, SoPh, 274, 399, https://doi.org/10.1007/s11207-011-9758-x

Feigelson, E. D. 1997, in Astronomical Time Series, ed. D. Maoz, A. Sternberg, & E. M. Leibowitz (Dordrecht: Springer)

Ge, Z. 2007, AnGeo, 25, 2259, https://doi.org/10.5194/angeo-25-2259-2007

Gilman, D. L., Fuglister, F. J., & Mitchell Jr., M. M. 1963, JAtS, 20, 182, https://doi.org/10.1175/1520-0469(1963)020<0182:OTPSON>2.0.CO;2

Grinstead, J. W., Wang, D., Bhat, H., et al. 2014, Proc. Intl. Soc. Mag. Reson. Med., 22

Heiken, G. H., Vaniman, D. T., & French, B. M. 1991, Lunar Sourcebook, A User's Guide to the Moon, (Cambridge, MA: CUP)

Jenniskens, P. 1998, EP&S, 50, 555, https://doi.org/10.1186/BF03352149

Jopek, T. J. & Kaňuchová, Z. 2017, P&SS, 143, 3, https://doi.org/10.1016/j.pss.2016.11.003

Jorgensen, J. L., Benn, M., Connerney, J. E. P., et al. 2020, JGR Planets, 126, e2020JE006509, https://doi.org/10.1029/2020JE006509

Karttunen, H., Kröger, P., Oja, H, Poutanen, M. & Donner, K. J. 2017, Fundamental Astronomy (Berlin: Springer-Verlag), https://doi.org/10.1007/978-3-662-53045-0

Korotev, R. L. & Irving, A. J. 2021, M&PS, 56, 206, https://doi.org/10.1111/maps.13617

Maravilla, D., Arenas-Alatorre, J., & Cañetas-Ortega, J. 2013, J. Adv. Microsc. Res., 8, 252, https://doi.org/10.1166/jamr.2013.1166

Mas Sanz, E., Trigo Rodríguez, J. M., Silber, E. A., et al. LPSC, 51, 2155

McKay, D. S., Gibson Jr., E. K., Thomas-Keprta, K. L., et al. 1996, Sci, 273, 924, https://doi.org/10.1126/science.273.5277.924

McSween Jr., H, Y. 1996, M&PS, 31, 691, https://doi.org/10.1111/j.1945-5100.1996.tb02045.x

Mendoza, B., Velasco, V. M., & Valdés-Galicia, J. F. 2006, SoPh, 233, 319, https://doi.org/10.1007/s11207-006-4122-2

Moorhead, A. V, Kingery, A., & Ehlert, S. 2020, JSpRo, 57, 160, https://doi.org/10.2514/1.A34561

Mursula, K. & Zieger, B. 1996, JGR, 101, 27077, https://doi.org/10.1029/96JA02470

Prabhakaran Nayar, S. R., Nair, V. S., Radhika, V. N., & Revathy, K. 2001, SoPh, 201, 405, https://doi.org/10.1023/A:1017599621110

Prabhakaran Nayar, S. R., Radhika, V. N., Ramadas, V., & Revathy, K. 2002, SoPh, 208, 359, https://doi.org/10.1023/A:1020565831926

Prabhakaran Nayar, S. R., Alexander, L. P., Radhika, V. N., et al. 2004, AnGeo, 22, 1665, https://doi.org/10.5194/angeo-22-1665-2004

Peña-Asensio, E., Trigo-Rodríguez, J. M., Josep, M., & Rimola, A. 2022, AJ, 164, 76, https://doi.org/10.3847/1538-3881/ac75d2

Rubin, A. E. & Grossman, J. N. 2010, M&PS, 45, 114, https://doi.org/10.1111/j.1945-5100.2009.01009.x

Scargle, J. D. 1997, in Astronomical time series, ed. D. Maoz, A. Sternberg, & E. M. Leibowitz (Dordrecht: Springer)

Singh, Y. P. & Badruddin 2014, P&SS, 96, 120, https://doi.org/10.1016/j.pss.2014.03.019

Soon, W., Dutta, K., Legates, D. R., Velasco, V., & Zhang, W. 2011, JASTP, 73, 2331, https://doi.org/10.1016/j.jastp.2011.07.007

Soon, W., Velasco Herrera, V. M., Cionco, R. G., et al. 2019, MNRAS, 483, 2748, https://doi.org/10.

1093/mnras/sty3290
Tagliaferri, E., Spalding, R., Jacobs, C., Worden, S. P., & Erlich, A. 1994, in Hazards due to comets and asteroids, ed. T. Gehrels, M. S. Matthews, & A. Schumann (Arizona, AZ: UAP)
Torrence, Ch. & Compo, G. P. 1998, BAMS, 79, 61, https://doi.org/10.1175/1520-0477(1998)079<0061:APGTWA>2.0.CO;2
Trigo-Rodríguez, J. M., Madiedo, J. M., Gural, P. S., et al. 2008, in Advances in Meteoroid and Meteor Science, ed. J. M. Trigo-Rodríguez, F. J. M. Rietmeijer, J. Llorca, & D. Janches (New York, NY: Springer)
Trigo-Rodríguez, J. M. & Blum, J. 2009, PASA, 26, 289, https://doi.org/10.1071/AS08070
Trigo-Rodríguez, J. M. 2019, in Hypersonic meteoroid entry physics, ed. G. Colonna, M. Capitelli, & A. Laricchiuta (Bristol, UK: IOP Publishing)
Trigo-Rodríguez, J. M. & Blum, J. 2022, MNRAS, 512, 2277, https://doi.org/10.1093/mnras/stab2827
Velasco Herrera, V. M., Soon, W., Velasco Herrera, G., Traversi, R. & Horiuchi, K. 2017, NewA, 56, 86, https://doi.org/10.1016/j.newast.2017.04.012
Vernazza P., Marset M., Beck, P., et al. 2015, ApJ, 806, 204, https://doi.org/10.1088/0004-637X/806/2/204
Williams I. P. 2002, in Meteors in the Earth's atmosphere, ed. E. Murad & I. P. Williams (Cambridge, UK: CUP)



G. Cordero and D. Maravilla: Instituto de Geofísica, Universidad Nacional Autónoma de México, (dmaravil@igeofisica.unam.mx).
M. Pazos: Instituto de Cambio Climático, y Ciencias de la Atmósfera, UNAM, México.